ELSEVIER

Journal of Crystal Growth 149 (1995) 187–195

JOURNAL OF CRYSTAL GROWTH

Extremely flat surfaces by liquid phase epitaxy

A.A. Chernov [a,b,1], H.J. Scheel [b,*]

[a] *Institute of Crystallography, Russian Academy of Science, Leninsky Prospekt 59, 117333 Moscow, Russian Federation*
[b] *Cristallogenèse, Institut de Micro-et-Optoélectronique EPFL, Ch. de Bellerive 34, CH-1007 Lausanne, Switzerland*

Received 30 November 1993; manuscript received in final form 28 November 1994

Abstract

By analysis of liquid phase epitaxial (LPE) growth experiments of GaAs multilayer structures, the incorporation rates at elementary growth steps (kinetic coefficients) are estimated. Conditions are presented to prepare large singular surfaces with several micrometers distances between regular elementary steps. Such quasi atomically flat surfaces may become important for applications in semiconductor and superconductor technologies, in surface physics and catalysis, as reference planes, and also as substrates for fabrication of extremely homogeneous layers and perfect superlattices.

1. Introduction

Surface and interface flatness is an important factor in quantum electron devices [1], multilayer optical waveguides [2], and in tunnel junctions based on high-temperature superconductors with their very short coherence lengths [3]. Other applications of nearly step-free surfaces are in surface physics and in studies of the role of steps in catalysis. Further applications of extremely flat surfaces make use of the perfect homogeneity of layers and multilayers grown on these facets by the single-step-flow mode. This is explained by the sensitivity of the dopant incorporation to the surface topology: the distribution coefficient depends on the local step density [4], and bunched steps (macrosteps) give rise to striations [5,6]. On vicinal faces the density of macrosteps is increasing with the increasing angle of misorientation, and it is also influenced by supersaturation and by surface kinetics [4,7].

A number of techniques and approaches were tried to achieve flat surfaces. Physical vapor deposition methods like molecular beam epitaxy (MBE), sputtering, laser ablation, etc. may yield on average flat surfaces which, however, have high step densities. The mean distance between steps is 10–50 nm, and it is difficult to achieve inter-step distances of greater than 100 nm. The limits of MBE methods can also be explained in terms of non-equilibrium growth.

However, liquid phase epitaxy has the potential to achieve near-equilibrium growth on well-oriented surfaces with large interstep distances [6,8], rather than the step-flow mode at small step distances on vicinal surfaces [9–11]. This has been demonstrated by means of a sliding-free LPE technology [12] in multilayer LPE of Sn- and Ge-doped GaAs onto slightly misoriented sub-

* Corresponding author.

[1] The work was performed during a visiting professorship of A.A.C. at EPF Lausanne, Switzerland.

SSDI 0022-0248(95)00014-3

strates. The spreading of the facet at the expense of the adjacent vicinal surface was observed [6] whereby simultaneously the number of growth hillocks was reduced. Typically, one or two growth centers were observed, either at the rim or near the center of the facet, and thus the activity of the other screw dislocations was suppressed. The facets showed a regular sequence of steps of 0.65 nm height [13] and a mean step separation of 6 μm. These singular F facets [15] are close to equilibrium, in the sense of Gibbs, Wulff and Herring [14]. In other words, the near-equilibrium slider-free LPE growth allows macroscopically flat surfaces and interfaces.

In this paper the earlier LPE experiments of Scheel [6] are analyzed to evaluate the kinetic coefficient for steps in LPE of GaAs in Section 2. The time-dependence of the transformation to facets is derived in Section 3. In Section 4 the experimental conditions required for achieving large facets with minimum step density are discussed.

2. Growth modes and kinetic coefficient for steps

The estimation of the kinetic coefficient for steps in LPE-grown GaAs is based on earlier experiments. The multilayer structures of alternating p- and n-GaAs [6] have been angle-lapped and etched in order to reveal the surface topology at the edge E between the facet F and the misoriented stepped surface S. This is schematically shown for two subsequent positions of the interface in Fig. 1. The growth velocities R_F and R_S of the facet and of the stepped surface are taken perpendicular to the singular crystallographic plane. In two experiments, the angle p_S between the F- and S-faces was 0.165° (2.9×10^{-3} rad) for experiment L17A and 0.573° (10^{-2} rad) for experiment L19B. The facet itself has an extremely small misorientation with the crystallographic [111] direction, namely ~ 20 seconds corresponding to 1.1×10^{-4} rad given by the regular train of elementary steps of 6.5 Å height [13] and 6 μm mean interstep distance.

The noticeable growth rate ratios R_S/R_F of 1.5 for L17A and 1.7 for L19B, rather than

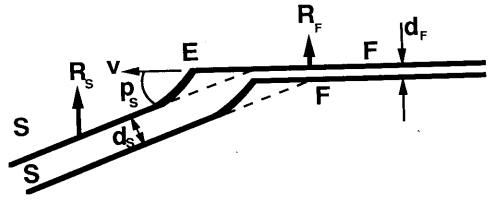

Fig. 1. Schematic view of two successive stages of the growth surface near the edge E between the stepped surface S and the facet F. The angle p_S between the S- and F-surfaces as well as the growth rates R_S, R_F and layer thicknesses d_S, d_F are indicated.

$R_S/R_F = 1$ indicate that the growth of the facet is at least partially limited by surface kinetics, whereas for the S-face the diffusion limited regime is expected. The thickness d_S of the layers grown on the S-face may be derived from the standard relationship [16,17]

$$d_S = d_{S1} + d_{S2} = 2\left(\frac{\Delta T}{C_S}\frac{\partial C_e}{\partial T}\right)\left(\frac{D}{\pi}\right)^{1/2} t^{1/2} + \frac{3}{2}\left(\frac{\dot{T}}{C_S}\frac{\partial C_e}{\partial T}\right)\left(\frac{D}{\pi}\right)^{1/2} t^{3/2}, \quad (1)$$

where d_{S1} and d_{S2} are the thicknesses due to the initial undercooling ΔT and the permanently decreasing temperature $\dot{T} = dT/dt$, t being the time. Taking the data of the equilibrium concentration of As in Ga solution at 820°C $C_e = 2.6$ at % $= 1.32 \times 10^{21}$ cm^{-3}, $\partial C_e/\partial T = 1.12 \times 10^{19}$ cm^{-3} K^{-1}, the As concentration in the GaAs crystal $C_S = 2.2 \times 10^{22}$ cm^{-3}, the diffusivity $D = 5 \times 10^{-5}$ cm^2/s, the experimental parameters $\Delta T = 1.7$ K, $\dot{T} = 3.5$ K/h and the growth time per layer $t = 600$ s, one obtains from Eq. (1) $d_{S1} = 1.7$ μm, $d_{S2} = 0.43$ μm and thus $d_S = 2.13$ μm. This value should be compared with the measured value of 2.44 μm for the first layer and an average layer thickness of 2.3 μm. A more precise calculation is meaningless since the loss of As vapor during the experiment was not measured. Nevertheless, we may conclude from the layer geometry and the above estimation that the stepped surfaces grow in the diffusion-limited regime whereas the growth rate of the facets is

partially controlled by surface incorporation kinetics.

From the above experimental data one can estimate the kinetic coefficients β_{st} of an elementary step and β of a stepped surface. These coefficients are defined as factors of proportionality between the step or the S-face growth rates, v or R, respectively, and the dimensionless driving force $\Delta\mu/kT$ for crystallization immediately at the step or at the interface, respectively:

$$v = (C/C_S)\beta_{st}\Delta\mu/kT;$$
$$R = (C/C_S)\beta\Delta\mu/kT. \quad (2)$$

Here $\Delta\mu$ is the chemical potential difference of the crystallizing species in the solution and in the crystal, and C is the solute concentration at the step or at the surface. We assume $C < C_S$, and the ratio C/C_S corresponds to the probability of finding the crystallizing species just at the step or at the surface site, whereas the kinetic coefficients represent the average incorporation rates. For dilute solutions like As in Ga, $C/C_S \ll 1$. As a first approximation the relative supersaturation $(C - C_e)/C_e = \Delta\mu/kT$ thus giving

$$C_S v = \beta_{st}(C - C_e); \qquad C_S R = \beta(C - C_e). \quad (3)$$

The mass conservation law at the step and at the interface gives

$$D\,\partial C/\partial r = (C_S - C)v = (1 - C/C_S)\beta_{st}(C - C_e), \quad (4)$$

and

$$D\,\partial C/\partial n = (C_S - C)R = (1 - C/C_S)\beta(C/C_e). \quad (5)$$

Here the step is considered as a cylindrical sink, and $\partial C/\partial r$ in Eq. (4) is the radial derivative taken at an effective radius of the order of the step height. Similarly, $\partial C/\partial n$ is the derivative with respect to the normal to the interface.

According to the step height $h = 6.5$ Å the parameter [18] $(\beta_{st}h/\pi D)\ln|p| \ll 1$, and thus the kinetic coefficient β for the vicinal face, declined from the singular orientation by a small angle (say with the tangent $p \approx 1.1 \times 10^{-4}$ in experiment L17A) is just

$$\beta = \beta_{st}|p|. \quad (6)$$

Since the precise dependencies of the facet growth rate R_F on supersaturation and on time are not known, we assume for simplicity a linear approximation of the concentration within the boundary layer δ, and the corresponding growth rate is, by using Eqs. (5) and (6),

$$R = \frac{C_\delta - C_e}{C_S - C_e}\,\frac{1}{1/\beta_{st}p + \delta/D}. \quad (7)$$

Here C_δ is the concentration in the bulk liquid in contact with the boundary layer of thickness δ, and the modulus symbol used in Eq. (6) is omitted. The ratio R_S/R_F obtained from Eq. (7) for the face F, $p = p_F$, and S, $p = p_S$, gives

$$\frac{\beta_{st}\delta}{D} = \frac{(R_F/p_F) - (R_S/p_S)}{R_S - R_F}. \quad (8)$$

Taking $p_F = 1.1 \times 10^{-4}$ for both experiments L17A and L19B (although these values should slightly differ), and $p_S = 2.9 \times 10^{-3}$ and 10^{-2}, and the measured growth rates R_S and R_F from Ref. [6], one gets

$$\beta_{st}\delta/D \approx 1.3 \times 10^4 \text{ and } 1.7 \times 10^4. \quad (9)$$

Table 1
Kinetic coefficients for growth from solutions and from melts

Growth system	Density ratio [a]	β_{st}^T, β^T [b] (cm/s · K)	β_{st}, $\beta_{st}^T kT/\Delta S$ (cm/s)	Ref.
Aqueous solution	0.03–0.3		10^{-3}–10^{-1}	[20,21]
Flux growth and LPE of garnets	0.2–0.3		10^{-3}	[22–24]
Si from melt (T_m = 1687 K; $\Delta S/k$ = 2.83)	0.91	50	3×10^4	[25]
Pb from melt (T_m = 600 K; $\Delta S/k$ = 1.03)	0.94	28.7	1.7×10^4	[19]
LPE of GaAs	0.06		1–10	This work
YBCO	0.05		$\sim 10^{-2}$	Estimate, this work

[a] Density ratio = density of crystallizing species in solution/density of the species in the crystal.
[b] For melts.

With $\delta = 2\sqrt{Dt} = 0.35$ cm ($D = 5 \times 10^{-5}$ cm^2/s, $t = 600$ s) and 0.24 cm ($t = 300$ s) the values of Eq. (9) give $\beta_{st} = 2$ and 4 cm/s for experiments L17A and L19B, respectively. Thus a value of $\beta_{st} = 3$ cm/s may be taken as a first estimate of the step kinetic coefficient. In these LPE experiments a modest forced convection was applied by oscillatory rotation of the container. The reduced effective boundary layer thickness would lead to a larger value of β_{st} of about 10 cm/s. For a more accurate determination of β_{st} and $\beta = \beta_{st}|p|$, one would need experimental data at various supersaturations in order to obtain the expected non-linear dependence of the facet growth rate R_F on the supersaturation at the growing interface.

Our estimated values of $\beta_{st} \approx 1$–10 cm/s for growth of GaAs from Ga solution should be compared with other systems. This is done in Table 1 where data of different systems of growth from solutions and from melts are given. In the latter case the atomically rough interface and the step have similar kinetic coefficients $\beta_{st}^T \approx \beta^T$. The coefficients β_{st}^T and β^T for melt (cm/s · K) and β_{st}, β for solutions are related by the equation $\beta = (\beta_T^T/\Delta S)(C_s/C)$, where ΔS is the entropy of fusion. From the values given in Table 1 it can be seen that the kinetic coefficient for LPE-grown GaAs lies between the smaller values for growth from aqueous solutions and for flux growth of garnets on the one hand, and the much larger values for crystallization of Pb and Si from melts. This is understandable in view of the high desolvation barrier (10–20 kcal/mol) that an ion or molecule has to overcome to be incorporated in the lattice in growth from solutions. Noticeable changes in chemical bonding should be expected in oxide garnet systems as well. In analogy one would expect a similarly low kinetic coefficient also for high-T_c superconducting cuprates like $YBa_2Cu_3O_{7-x}$. In contrast, melt growth seems to be a barrier-free process [19,20]. The intermediate values of β_{st} for GaAs show that for the growth from Ga solution a potential barrier for incorporation into the crystal still exists, although it is lower than that for growth from aqueous solutions where the solvent is not incorporated in the crystal.

3. Faceting time

For practical applications, i.e. for fabrication of facets of large size L, it is worth knowing the required time t_L. This time is derived in the following for the stagnant solution with the diffusion-limited growth regime of the S-face, and for the stirred solution where bulk diffusion is assumed to be negligible.

3.1. Stagnant solution

The edge E moves along the face F with the rate [4] (see Fig. 1)

$$v = (R_S - R_F)/(p_S - p_F). \tag{10}$$

Since p_S and p_F are time independent one has

$$L = \int_0^{t_L} v\,dt = [d_S(t_L) - d_F(t_L)]/(p_S - p_F) \approx [d_S - d_F]/p_S. \tag{11}$$

The last approximate equality in Eq. (11) is valid since $p_F \ll p_S$. The function $d_S(t)$ is given by Eq. (1). To find $d_F(t)$ the solution of the non-steady-state diffusion equation with the non-linear boundary condition at the facet growing by the screw-dislocation (or by the two-dimensional nucleation) mechanism should be found. Instead, we used in the Appendix the quasi-steady-state linear approximation, which was already employed to obtain Eq. (7), and got as result

$$L = 2p_S^{-1}d_0\int_0^1 \left[\sqrt{1 + \left(\chi\Delta T + \tfrac{9}{4}\chi\dot{T}t\right)t^{1/2}} - 1\right]\frac{dt}{t}, \tag{12}$$

with d_0 and χ defined by Eqs. (A.5).

The estimate with $\beta_{st} = 2$ cm/s, $h = 6.5$ Å, $kT = 1.5 \times 10^{-13}$ erg, $\omega = 4.54 \times 10^{-23}$ cm^3, $\alpha = 300$ erg/cm^2, $D = 5 \times 10^{-5}$ cm^2/s, $C_e = 1.32 \times 10^{21}$ cm^{-3}, $\partial C_e/\partial T = 1.12 \times 10^{19}$ cm^{-3} K^{-1} and $p_S = 10^{-4}$ gives $\chi \approx 0.6$ K^{-1} s$^{-1/2}$. For $\Delta T = 0$ the time-dependent part in brackets under the square root of Eq. (12) does not exceed unity except for $t^{3/2} < 4/(9\chi\dot{T})$. For this inequality with $\dot{T} = 10^{-3}$ K/s = 3.6 K/h the time $t < 10^2$ s is needed. Even shorter times may be considered as an initial growth period if $\dot{T} = 0$ and ΔT is of

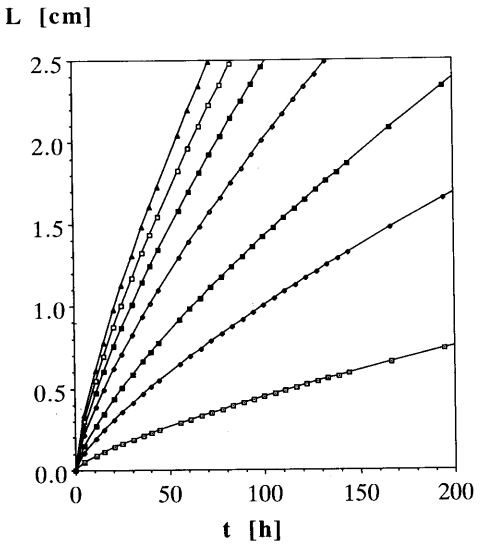

Fig. 2. Development of the facet size L with time according to Eq. (14), using the parameters given in the text, for various cooling rates at a fixed angle $p_S = 0.1°$. (⊡) $dT/dt = 0.1$ K/h; (♦) $dT/dt = 0.5$; (■) $dT/dt = 1$; (◆) $dT/dt = 2$; (■) $dT/dt = 3$; (□) $dT/dt = 4$; (▲) $dT/dt = 5$.

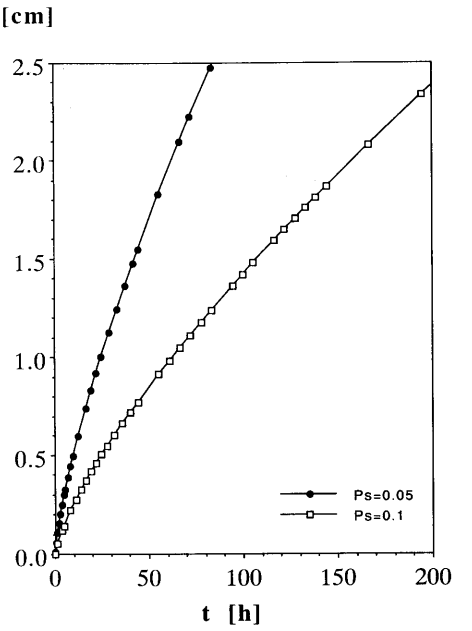

Fig. 3. Facet development for a fixed cooling rate of 1 K/h and two misorientation angles $p_S = 0.05°$ and 0.1° (same parameters as Fig. 2).

the order of several K. However, the most interesting part of the solution is the long-term experiments needed to obtain large facet size L.

In this case, if

$$\chi \Delta T t^{1/2} + \tfrac{9}{4}\chi \dot{T} t^{3/2} \gg 1 \text{ and } t \gg \Delta T/\dot{T}, \qquad (13)$$

Eq. (12) gives

$$L = 6 d_0 \chi \dot{T} t^{3/4}$$

$$= \frac{2\omega}{p_S}\left(\frac{19\omega C_e \alpha \dot{T}}{\beta_{st} hkT}\frac{\partial C_e}{\partial T}\right)^{1/2}\left(\frac{Dt}{\pi}\right)^{3/4}. \qquad (14)$$

With the values used above, Eq. (14) gives

$$L = 3.2 \times 10^{-7} t^{3/4}\ (\text{s})/p_S\ (\text{cm}). \qquad (15)$$

Thus, at $\dot{T} = 10^{-3}$ K/s = 3.6 K/h, the facet of 4 cm length needs about 10 days growth time. Although such long experiments are possible, one would like to shorten the time for practical reasons. Graphic presentations of Eq. (14) with the system parameters defined above are shown in Figs. 2–4. In Fig. 2 the Burgers vector for the steps on the facet is taken as $2d_{(111)} = 6.5$ Å, and

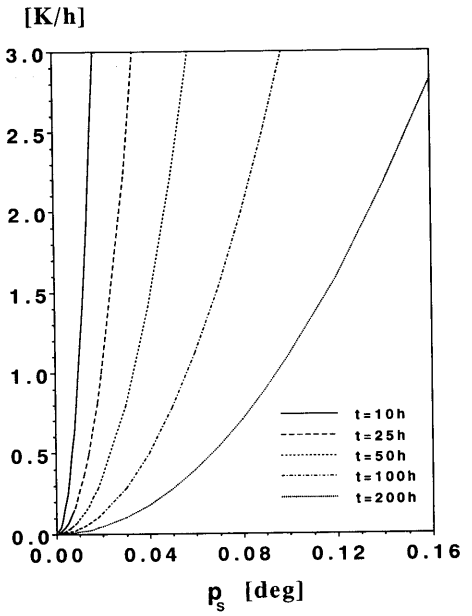

Fig. 4. Curves representing different times required to develop a facet of size $L = 2.5$ cm as a function of cooling rate $\dot{T}$ and misorientation angle p_S (same parameters as Fig. 2).

the misorientation angle is fixed at $p_S = 0.1°$. The times t to arrive at the facet sizes L are reduced at higher cooling rates as long as 2D-nucleation and step bunching are prevented, up to about 2 K/h. Above this supersaturation limit also the tendency to growth instability is increasing. Fig. 3 shows for a fixed cooling rate of 1 K/h the facet development for two different misorientation angles. The relation cooling rate and misorientation angle is presented in Fig. 4. Lines of equal times required to reach $L = 2.5$ cm are shown. Again, above about 2 K/h (for this specific growth system) the tendency to step bunching, 2D-nucleation, and growth instability is increasing. Approaches to fasten the spreading of the facet may be achieved by lowering the activity of the step source by, for example, dislocations possessing elementary Burgers vectors rather than larger ones (quantity h in Eq. (14)). The same measure would prevent step bunching. If the facet were dislocation-free, and the supersaturation would be kept below the level needed for 2D-nucleation, then R_F would be negligibly small, and with $d_F = 0$ one would have from Eq. (11)

$$L = \frac{d_S}{p_S}, \tag{16}$$

with d_S obeying Eq. (1). An example of a practical solution is epitaxial lateral overgrowth [26] by liquid phase epitaxy. Another approach consists of reducing the diffusional limitation of the growth rate of the stepped surface, and this is discussed in the next section.

3.2. Forced convection

From the various stirring techniques in LPE [27] the rotating substrate is the most advantageous. The analysis of the flow towards the rotating disc by Cochran [28] and the study of the distribution relations by Burton, Prim and Slichter [29] have established a uniform diffusion-boundary-layer thickness which can be adjusted by the rotation rate. When the step density of the facet p_F is known the growth rates R_F and R_S can be estimated from Eq. (7). For low supersaturations corresponding to $R_F \ll R_S$ one arrives at the most favorable condition Eq. (16), with the supersaturation

$$\sigma_\delta \ll 19\omega\alpha D/\delta\beta_{st}hkT. \tag{17}$$

With the parameters given above, and assuming

$\beta_{st} = 2$ cm/s, $\delta = 10^{-1}$ cm,

$\sigma_\delta = (C_\delta - C_e)/C_e = 10^{-3}$ and $p_S = 10^{-4}$,

one obtains

$$L = D\omega C_e\sigma_\delta t/p_S\delta \approx 3 \times 10^{-4}t \text{ (cm)}. \tag{18}$$

Thus, a facet of 10 cm diameter may be grown in less than one day.

The required low supersaturation can be achieved by programmed slow cooling of the solution, by material transport from a solid source in a temperature gradient, or for volatile components (As in the case of GaAs) by transport via the gas phase. The programming of the supersaturation should take into account that with increasing size of the facet relative to the stepped part of the surface the rate of solute precipitation has to be reduced accordingly during the experiment.

4. Experimental conditions to achieve large facets

From the foregoing discussions one can derive the theoretically expected requirements for the technical realisation of extended faceted surfaces of excellent flatness by epitaxial layer deposition: homoepitaxy is preferred, and in case of heteroepitaxy the *misfit* between substrate and layer has to be extremely small ($\ll 0.2\%$) in order to achieve the *Frank–Van der Merwe layer-by-layer growth mode*. To minimize the step density, growth conditions excluding two-dimensional nucleation should be applied. In view of a significant layer thickness required to achieve the spreading of a large facet, the misfit has to be small enough to prevent cracking and propagation of cracks. If misfit dislocations are to be avoided the demands for low misfit become even more stringent. Also the *thermal expansion coefficients* of substrate and layer should be similar to avoid cracking and bending of the surface.

Another requirement is based on the fact that the rate of facet spreading is inversely propor-

tional to the misorientation angle. Thus, one needs a specific *small misorientation* of the initial substrate surface, as with large misorientations of say more than 0.2° or 0.3°, the time to achieve complete faceting becomes excessively long. Similarly a sufficiently *high growth rate* is required under growth conditions where the facet still continues to grow in the regular step-flow mode and is thermodynamically stable. In growth from melts this might be achieved for solids with large α- (Jackson) or γ- (Temkin) factors at sufficiently low thermal gradients. For high-melting point semiconductors and for oxide compounds (with applications in optics, magnetics and superconductivity) the most promising approach is *liquid phase epitaxy*. In LPE the spreading of the facet is facilitated for the proper crystallographic orientations by the near-equilibrium growth conditions, and the growth rates in LPE are – depending on solute concentration and growth temperature – sufficiently high, typically 50–500 Å/s. For unconstrained growth of the required layer thickness, a sliding-free LPE technology is to be used, be it the tilting boat of Nelson (1963) or a rotating immersed substrate, or the slider-free multilayer LPE process by which 3 mm facets had been achieved in 1980 [6].

Also in *growth from the vapor phase* the crystals are normally faceted so that it can be assumed that the transition to faceting can also be achieved in vapor phase epitaxy (VPE), chemical vapor deposition (CVD) and in metalorganic chemical vapor deposition (MOCVD). The challenge here would be to establish sufficiently high growth rates below the supersaturation limit for two-dimensional nucleation. This is expected to be even more difficult in physical deposition methods involving vacuum like MBE, sputtering, etc. In these cases, generally two-dimensional nucleation and local step flow are observed on substrates near to the singular orientation, whereas misoriented surfaces may provide pure step flow at high step densities. The development of large facets with small step density in MBE-like techniques is hampered also by the very low deposition rates of typically 1 Å/s.

In the absence of two-dimensional nucleation, there has to be a source of steps like simple screw dislocations, multiple dislocation arrays or other complex defects. In the earlier LPE experiments [6] it was realized that during the growth of p–n-GaAs multilayers the dislocation density of the original substrate of $(2–5) \times 10^4$ cm^{-2} was significantly reduced or at least no more active at the surface. It was not investigated whether the reduction of hillocks was due to annihilation or due to bending outwards of dislocations caused by strain fields at macrosteps, or both, or whether at low supersaturation the simple step sources have become inactive since surface nucleation is dominated by defects with large Burgers vectors. In any case it would be desirable in facet fabrication to achieve defined step sources with small Burgers vectors, and to prevent step bunching.

5. Conclusions

The analysis of LPE experiments of GaAs showed that the (111) facet is spreading even in the partially diffusion-controlled regime. The kinetic coefficient for elementary steps on the GaAs (111) surface was estimated for the first time. The value of $\beta_{st} \approx 1–10$ cm/s lies between the values $10^{-3}–10^{-1}$ cm/s for growth of salts from aqueous solutions and of garnets from flux, and the values of 10^4 cm/s for growth of elements (Si, Pb) from the melt. The estimated kinetic coefficient allowed a derivation of the time required to obtain large (~ 10 cm) singular surfaces with very low step densities as a function of substrate misorientation and supersaturation. This growth time of typically several days for the diffusion-limited growth regime can be reduced to less than one day when effective stirring (e.g. rotation of the substrate) is applied. For achieving a very low step density, with a step separation of several micrometers, the supersaturation should not pass an upper limit where two-dimensional nucleation sets in. In LPE the supersaturation can be achieved by slow cooling, by material transport in a temperature gradient, or in the case of GaAs by transport of As in the gas phase. However, also vapor phase epitaxy like MOCVD may be attempted to achieve large facets.

The large crystallographically strictly oriented

surfaces with very low step density can be achieved not only on semiconductors, but also on metals, superconductors, oxide compounds, etc. Thus, these facets will be useful in surface physics and surface chemistry, as reference surfaces, but also in several device areas where flat surfaces and interfaces are important. As examples we mention semiconducting and superconducting tunnelling devices and multilayer optical waveguides. Furthermore, substrates with these quasi ideally flat surfaces may be used to grow highly homogeneous layers and superlattices free of striations caused by step bunching.

Acknowledgments

The authors thank Professors M. Ilegems, W. Kurz and T. Ring for support and Miss Chr. Klemenz for preparing the plots and creative collaboration.

Appendix

We assume that first the Ga and As species are directly incorporated at the steps [21] generated by screw dislocations [6,13], and second that the cooling rate is responsible for the growth features, thus neglecting the initial supercooling. Then, the quasi-steady-state approximation (c.f. Eq. (7)) with the boundary layer $\delta = \sqrt{\pi D t}$ gives

$$\sigma = \frac{\sigma_\delta}{1 + (\beta_{st} p \delta / D)}, \qquad p_F = \frac{hkT\sigma}{19\omega\alpha}, \tag{A.1}$$

from which one gets:

$$\sigma = \left(\sqrt{1 + 4q\sigma_\delta} - 1\right)/2q,$$

$$q \equiv \beta_{st}\delta hkT/19D\omega\alpha, \qquad \delta = \sqrt{\pi D t}. \tag{A.2}$$

The growth rate of the facet is

$$R_F = \beta_{st} p_F \omega C_e \sigma. \tag{A.3}$$

Thus the thickness of a layer deposited on the facet is

$$d_F(t) = \int_0^t R_F \, dt$$

$$= d_0 \int_0^t \left[\sqrt{1 + \chi\left(\Delta T + \tfrac{9}{4}\dot{T}t\right)t^{1/2}} - 1\right]^2 \frac{dt}{t}$$

$$= d_S - 2d_0 \int_0^t \left[\sqrt[4]{1 + \chi\left(\Delta T + \tfrac{9}{4}\dot{T}t\right)t^{1/2}} - 1\right] \frac{dt}{t}, \tag{A.4}$$

with

$$d_0 \equiv \frac{19\omega^2 C_e \alpha D}{4\pi\beta_{st} hkT}; \qquad \chi \equiv \frac{4\beta_{st} hkT}{19\omega C_e \alpha}\sqrt{\frac{\pi}{D}}\frac{\partial C_e}{\partial T}, \tag{A.5}$$

with d_S obeying Eq. (1).
Eq. (A.4) is substituted into Eq. (11) of the main text and gives Eq. (12).

References

[1] F. Capasso, Ed., Physics of Quantum Electron Devices (Springer, Berlin, 1990).
[2] S. Kondo, S. Miyazawa and H. Iwasaki, Mater. Res. Bull. 15 (1980) 243.
[3] A.I. Braginski, in: Toward a Technology of Electronic Circuits with High-T_c Superconductors, Proc. SQUID 1991, in press.
[4] A.A. Chernov, Modern Crystallography III: Crystal Growth, Springer Series Solid State, Vol. 36 (Springer, Berlin, 1984).
[5] T. Kajimura, K. Aiki and J. Umeda, Appl. Phys. Lett. 30 (1977) 526.
[6] H.J. Scheel, Appl. Phys. Lett. 27 (1980) 70.
[7] T. Nishinaga, K. Pak and S. Uchiyama, J. Crystal Growth 43 (1978) 85.
[8] R.C. Peters, Inst. Phys. Conf. Series 17 (1973) 55;
A. Mottram and A. R. Peaker, J. Crystal Growth 27 (1974) 193.
[9] K. Ishida, T. Kamejima and T.J. Matsui, Appl. Phys. Lett. 31 (1977) 397.
[10] D.L. Rode, W.R. Wagner and N.E. Schumaker, Appl. Phys. Lett. 30 (1977) 75.
[11] N. Toyoda, M. Mihara and T. Hara, Jap. J. Appl. Phys. 18 (1979) 2207.
[12] H.J. Scheel, J. Crystal Growth 42 (1977) 301.
[13] H.J. Scheel, G. Binnig and H. Rohrer, J. Crystal Growth 60 (1982) 199.
[14] C. Herring, in: Structure and Properties of Solid Surfaces, Eds. R. Gomer and C.S. Smith (University of Chicago Press, Chicago, 1953) p. 5.
[15] P. Hartman and W.G. Perdok, Acta Cryst. 8 (1955) 49, 521, 525.
[16] J.J. Hsieh, J. Crystal Growth 27 (1974) 49.
[17] G.B. Stringfellow, Rep. Progr. Phys. 45 (1982) 469.
[18] A.A. Chernov, J. Crystal Growth 24/25 (1974) 11.

[19] G.A. Rodway and J.D. Hunt, J. Crystal Growth 112 (1991) 554, 563.
[20] L.V. Mikheev and A.A. Chernov, J. Crystal Growth 112 (1991) 591.
[21] A.A. Chernov, Contemp. Phys. 30 (1989) 251.
[22] R. Ghez and E.A. Gless, Mater. Res. Bull. 8 (1973) 31.
[23] R.V. Telesnin, V.N. Dudorov and A.T. Morcherkov, Soviet. Phys.-Cryst. 21 (1976) 99.
[24] P. Görnert and F. Voigt, in: Current Topics in Materials Science, Vol. 11, Ed. E. Kaldis (Elsevier, New York 1984) p. 1.
[25] V.V. Voronkov, in: Crystals: Growth, Properties and Applications, Vol. 9, Modern Theory I (Springer, Berlin, 1983).
[26] S. Kinoshita, Y. Suzuki and T. Nishinaga, J. Crystal Growth 115 (1991) 561.
[27] D. Elwell and H.J. Scheel, Crystal Growth from High Temperature Solutions (Academic Press, London, 1975) ch. 8.
[28] W.G. Cochran, Proc. Cambridge Phil. Soc. 30 (1934) 365.
[29] J.A. Burton, R.C. Prim and W.P. Slichter, J. Chem. Phys. 21 (1953) 1987.